Following the failure of the third of six gyros, the system momentum test was enabled on November 20, 1992. With the test enabled, a soft gyro failure in a three-gyro configuration will trigger a safemode entry to either the Zero Gyro Sunpoint safemode in the flight computer or the hardware sunpoint capability using the Pointing and Safemode Electronics Assembly along with the retrieval mode gyros. The safety provided by the system momentum test will be even more critical if the HST is routinely operated in a three-gyro configuration after the first Hubble servicing mission, as is currently planned.

Acknowledgment

We acknowledge the seminal contribution of Henry Hoffman of the Goddard Space Flight Center in insisting on the fundamental importance of angular momentum conservation.

References

[1]Dougherty, H. J., Tompetrini, K., Levinthal, J., and Nurre, G., "Space Telescope Observatory in Space," *Journal of Guidance, Control, and Dynamics*, Vol. 5, 1982, pp. 403–409.

[2]Dougherty, H. J., Rodoni, C., Rodden, J., and Tompetrini, K., "Space Telescope Pointing Control," *Astrodynamics 1983, Advances in the Astronautical Sciences*, Vols. 54 I, II, American Astronautical Society, 1983, pp. 619–630.

[3]Beals, G. A., Crum, R. C., Dougherty, H. J., Hegel, D. K., Kelley, J. L., and Rodden, J. J., "Hubble Space Telescope Precision Pointing Control System," *Journal of Guidance, Control, and Dynamics*, Vol. 11, 1988, pp. 119–123.

[4]Markley, F. L., and Nelson, J. D., "A Zero-Gyro Safemode Controller for the Hubble Space Telescope," *Journal of Guidance, Control, and Dynamics* Vol. 17, 1994, pp. 815–822.

[5]Moy, E. W., and Kennedy, K. R., "Development of System Momentum Test for Zero Gyro Sunpoint," Lockheed Missiles and Space Co., Engineering Memorandum SPS 672, Sunnyvale, CA, Feb. 1992.

Pointing Dynamics of Gimbaled Payloads on Flexible Spacecraft

Bruno Marco Quadrelli*
Georgia Institute of Technology, Atlanta, Georgia 30332
and
Andreas H. von Flotow†
Hood Technology Company, Hood River, Oregon 97031

Introduction

IMPORTANT to certain missions is to point a small, rigid instrument gimbaled to a host spacecraft using gimbal torquers as actuators. If the gimbal torquers are perfect torque actuators (free of friction, backlash, elasticity, and other real effects) and if the gimbal axis passes through the payload mass center and is parallel to a payload principal axis of inertia, then the payload pointing dynamics will be unaffected by host spacecraft dynamics. The host spacecraft will be, of course, disturbed by the gimbal torques. The more common situation has the gimbal axis neither parallel to a payload inertia axis nor passing through the payload mass center. In addition, the gimbal axis may not be aligned with any of the principal axes of the spacecraft. In this case, the payload pointing dynamics (the transfer function from gimbal torque to payload inertial attitude angle) reflect the dynamics of the host spacecraft even with perfect torque actuators. This Note offers a simple derivation for this coupling and applies it to an example. In the case of low-mass or near-CG (center of gravity)-mounted payload, we show that the payload pointing dynamics are only slightly perturbed by host spacecraft dynamics. In particular, each spacecraft flexible mode contributes one nearly canceling pole-zero pair to the payload pointing transfer function. Reference 1 has studied the use of gimbal reactuation, in which gimbal torques are reacted, not against the host spacecraft, but against a reaction wheel mounted within the gimbal. This Note shows that such reactuation can help reduce the coupling but may also strengthen it.

Received May 20, 1992; revision received Nov. 5, 1993; accepted for publication Nov. 6, 1993.

*Graduate Student, Department of Aerospace Engineering. Member AIAA.

†President. Member AIAA.

Analysis

To see how the spacecraft flexibility influences in general the pointing dynamics of an articulated body of much smaller size mounted on it, consider the general two-dimensional system depicted in Fig. 1. The payload inertial angle is θ. The gimbal torque is τ. The gimbal constraint force perpendicular to the payload reference line u is F_v, and v is the corresponding inertial displacement. The payload moment of inertia about the center of mass is J, its mass is m, and the distance to the mass center from the gimbal axis is d. Assume also that the gimbal couples the payload and the spacecraft through a one-degree-of-freedom joint and that all motion is within the plane. We derive here the relevant linear equations of motion, based upon the assumption of small perturbations away from the reference configuration. The analysis includes both flexible and rigid-body motion.

The equilibrium of torques about the payload CG gives

$$\tau - F_v d = J\ddot{\theta} \tag{1}$$

The equilibrium of forces in the v direction is

$$F_v = m(\ddot{v} + d\ddot{\theta}) \tag{2}$$

and the relevant admittance relationship for the planar response of the spacecraft, not loaded by the payload, can be written as

$$\begin{pmatrix} \ddot{v} \\ \ddot{\theta} \end{pmatrix} = \begin{bmatrix} H_{vv} & H_{v\theta} \\ H_{\theta v} & H_{\theta\theta} \end{bmatrix} \begin{pmatrix} -F_v \\ \tau \end{pmatrix} \tag{3}$$

Combining these three equations in the frequency domain, one gets the following expression for the transfer function from torque t to inertial angle q:

$$\frac{\theta(s)}{\tau(s)} = \frac{(1 + mH_{vv}) + mdH_v\theta}{J(1 + mH_{vv}) + md^2} \frac{1}{s^2} \tag{4}$$

This expression shows where the spacecraft flexibility appears and also tells us that its effect is negligible when m is very small (very light payload) or when $d = 0$ (CG-mounted payload). Basically, the difference between the flexible and rigid-body transfer functions depends on the ratio of the payload inertia to base-body inertia characteristics.

To analyze the contribution of an individual flexible mode, it is useful to expand the spacecraft admittances H_{vv} and $H_{v\theta}$ in a

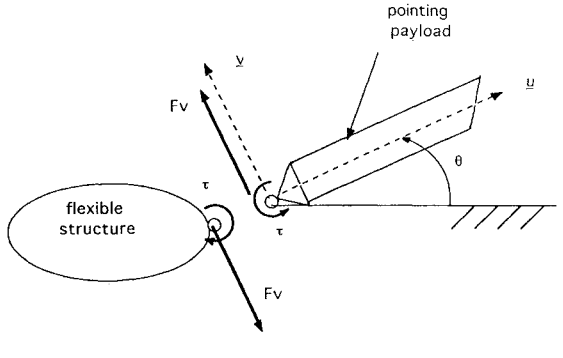

Fig. 1 Plane motion of a rigid payload gimbaled to a flexible spacecraft.

modal series. If we include modal damping ζ_i, these admittances take the form:

$$H_{vv} = \sum_{i=1}^{\infty} \frac{\Phi_i \Phi_i s^2}{m_i(s^2 + 2\zeta_i \omega_i s + \omega_i^2)}$$
$$H_{v\theta} = \sum_{i=1}^{\infty} \frac{\Phi_i' \Phi_i s^2}{m_i(s^2 + 2\zeta_i \omega_i s + \omega_i^2)} \tag{5}$$

where Φ_i and Φ_i' are the ith modal deflection in the v direction and slope about the gimbal axis at the mounting location and m_i is the modal mass for the ith mode of the flexible spacecraft, equal to $\Phi_i^T M \Phi_i$. We observe that the modes need not be mass normalized and that this series includes rigid-body modes, for which $\omega_i = 0$. Introduce now the quantities $\bar{m}_i = m_i/(\Phi_i \Phi_i)$ and $\bar{c}_i = m_i/(\Phi_i \Phi_i')$. They represent the inverse of the modal residues of the two transfer functions, the former with the dimensions of mass and always positive and the latter with the dimensions of first moment of inertia and not necessarily positive. At this stage we assume that the flexible modes of the host spacecraft are sufficiently spaced that we can consider each mode separately. Therefore, in the vicinity of the pth eigenfrequency, we have that, if j is the complex unit,

$$H_{vv} = \frac{s^2}{\bar{m}_p(s^2 + 2\zeta_p \omega_p s + \omega_p^2)} + \sum_{i=p+1}^{\infty} \frac{s^2}{\bar{m}_i \omega_i^2} + \sum_{i=1}^{p-1} \frac{s^2}{\bar{m}_i (j\omega_p)^2}$$
$$= \frac{s^2}{\bar{m}_p(s^2 + 2\zeta_p \omega_p s + \omega_p^2)} + (q_F - p_F) \tag{6}$$

where the positive numbers p_F and q_F represent the static contribution of, respectively, the lower modes including the rigid-body modes (inertia dominated) and the higher flexible modes (stiffness dominated). Similarly, we have

$$H_{v\theta} = \frac{s^2}{\bar{c}_p(s^2 + 2\zeta_p \omega_p s + \omega_p^2)} + (q_\tau - p_\tau) \tag{7}$$

where neither p_τ nor q_τ are necessarily positive.

If now we make the substitutions $A = m/\bar{m}_p$, $B = md/\bar{c}_p$, and $R = md^2/J$, we obtain

$$\frac{q(s)}{\tau(s)} = \frac{s^2[1 + (A + B)/C] + 2\zeta_p \omega_p s + \omega_p^2}{s^2[1 + (A/D)] + 2\zeta_p \omega_p s + \omega_p^2} \frac{C}{JDs^2} \tag{8}$$

where

$$C = 1 + m(q_F - p_F) + md(q_\tau - p_\tau)$$

and

$$D = [1 + m(q_F - p_F) + R]$$

This is an expansion, near the pth spacecraft eigenfrequency, of the transfer function from gimbal torque to inertial pointing angle. From this transfer function one can evaluate the expression of the resulting pole and zero as

$$P_{(1,2)} \cong (-\zeta_p \omega_p)\left(1 - \frac{A}{D}\right) \pm j\omega_p\left(1 - \frac{A}{2D}\right)$$
$$Z_{(1,2)} \cong (-\zeta_p \omega_p)\left(1 - \frac{A + B}{C}\right) \pm j\omega_p\left(1 - \frac{A + B}{2C}\right) \tag{9}$$

From these expressions, which are exact to first order in A and B, one can see that both the real part and the imaginary part of P and Z, and therefore the ordering along the imaginary axis and also the location with respect to the $-\zeta_p \omega_p$ line, change depending on the value of the parameters of the set $\{A, B, C, D, R\}$. The pole-zero spacing (neglecting the contribution of the adjacent modes) results in

$$\frac{(P - Z)_p}{\omega_p} \cong \frac{1}{2} \frac{B + R(A + B)}{1 + R} \tag{10}$$

which tends to zero when the payload is very light (since m, and thus A and B, tends to zero), when it is CG mounted (since B and R are zero), when the modal displacement and slope at the mounting location approach zero (since A and B approach zero), or in a very special case, if the numerator $B + R(A + B)$ is equal to zero.

The pointing transfer function, from gimbal torque to payload inertial angle, will thus exhibit pole-zero pairs near the eigenfrequencies of the flexible host spacecraft. The degree to which each pole-zero pair contributes gain and phase excursions to this transfer function depends upon their relative separation. If we define this separation to be

$$D_p = \frac{(P - Z)_p}{\omega_p} \tag{11}$$

then the resulting local phase excursion is[2]

$$D_\phi = -2\tan^{-1}\frac{D_p}{2\zeta} \tag{12}$$

and the local multiplicative gain excursion is[2]

$$M = \sqrt{1 + \left(\frac{D_p}{\zeta}\right)^2} \tag{13}$$

The magnitude of these local gain and phase excursions are thus seen to depend upon the ratio

$$\frac{1}{\zeta} \frac{B + R(A + B)}{1 + R} \tag{14}$$

which, remembering the definitions of the dimensionless parameters A, B, and R, scales in proportion to payload mass. This is an expected result. What might be less obvious is the ameliorating effect of passive damping revealed by the ratio (14).

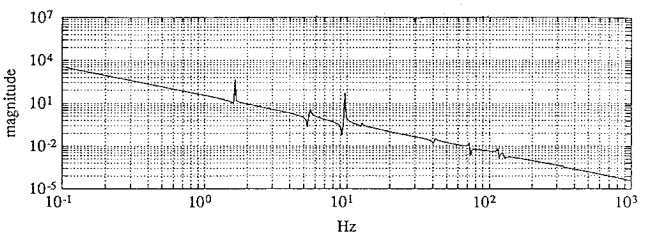

Fig. 2 Transfer function from gimbal torque to payload inertial angle.

Computed Example

For a system like the Space Shuttle's Middeck Active Control Experiment (MACE),[3] a multibody space structure being currently tested at Massachusetts Institute of Technology, the magnitude of the transfer function from gimbal torque to inertial pointing angle of one of the rigid payloads derived from a finite element model is shown in Fig. 2. The situation depicted is one of near pole-zero cancellation and shows that the effect of the flexible base upon the pointing dynamics is small. The payload, clearly, would behave like an independent rigid-body if the pole-zero cancellation was exact. The degree of pole-zero cancellation here is surprising, since the payload weighs about half as much as the host spacecraft.

Effect of Torque Reactuation

If the above analysis is repeated but pointing torques are "reactuated" into a gimbal reaction wheel rather than the host spacecraft (Ref. 1), then the coupling with the host spacecraft occurs only through the translational admittance H_{vv}. The pole-zero spacing, expression (10), then reduces to

$$\frac{(P-Z)_p}{\omega_p} \cong \frac{1}{2}\frac{RA}{1+R} \tag{15}$$

This pole-zero spacing may be greater, or less, than for the unreactuated case [Eq. (10)] depending upon the sign of the parameter B in Eq. (10). This is contrary to what is implied by the argument presented in Ref. 1, which was based upon a single simple example. What is clear from Eqs. (15) and (10) is that torque reactuation helps in achieving pole-zero cancellation of flexible host spacecraft dynamics only if B is positive; i.e., the spacecraft modal deflection (parallel to the direction v in Fig. 1) and the modal slope about the gimbal axis are of the same sign. There is no reason to expect this to be generally the case.

Extension to Three-Dimensional Case

Consider now the three-dimensional case, in which a general inertia distribution as well as a general offset of the CG are allowed for the articulated rigid-body. The articulation at the hinge is in this case defined by two angles. The displacement components are u, v, w. The inertia matrix J is a 3×3 matrix with nonzero off-diagonal elements, and the offset from a reference point on the gimbal axes to the payload mass center has three components. As before, one can define the parameters $A(i,j,k) = (m/\bar{m}_j)\Phi_i\Phi_k$, the parameters $B(i,j,k,l) = (md_l/\bar{c}_j)\Phi'_i\Phi'_k$, and the parameters $R(l,m,n) = md_l^2/J_{mn}$, where $(i,j) = u, v, w$ and $(l,m,n) = 1, 2, 3$. The set $\{A, B, C, D, R\}$, in this case, is of higher dimension. With such a large parameter set, it may be best to work directly with the three-dimensional equivalent of Eq. (4). This equation yields the 2×2 matrix of pointing transfer functions from a modal analysis of the host spacecraft not loaded with the payload. As in the two-dimensional case, one can examine the features of the dynamic coupling in the frequency domain in terms of the effect upon the pointing dynamics. The full analysis for the Space Shuttle's MACE is reported in Ref. 3.

Conclusions

This Note has discussed the transfer function from gimbal torque to inertial pointing angle of a dynamic system composed of a rigid articulated body mounted through a frictionless gimbal on a flexible spacecraft. This transfer function is shown to be slightly modified by spacecraft flexibility. The results of the analysis are useful in the design process. The idea of introducing a reactionless gimbal actuator, as proposed in Ref. 1, has also been revisited. A class of dimensionless parameters has been identified that defines the problem.

Acknowledgments

This research effort was partly supported by NASA contract NAS1-18690 from the National Aeronautics and Space Administration, Langley Research Center, with Mr. Anthony Fontana serving as Technical Monitor.

References

[1]Laskin, R. A., Kopf, R. H., Sirlin, S. W., Spanos, J. T., and Wiktor, P. J., "Reactionless Gimbal Actuator for Precision Pointing of Large Payloads," AAS Paper No. 87-512, 1987.

[2]Garcia, J. G., Sievers, L. A., and von Flotow, A. H., "High-Bandwidth Positioning Control of Small Payloads Mounted on a Flexible Structure," *Journal of Guidance, Control, and Dynamics*, Vol. 15, No. 4, 1992, pp. 928–934.

[3]Quadrelli, B. M., "Modeling, Dynamics Analysis and Control of a Multi-Body Space Platform," M.S. Thesis, Department of Aeronautics and Astronautics, Massachusetts Inst. of Technology, June 1992.

Performance Evaluation of Two Fuzzy-Logic-Based Homing Guidance Schemes

S. K. Mishra,* I. G. Sarma,† and K. N. Swamy‡
Indian Institute of Science, Bangalore 560012, India

Introduction

IN this Note, homing guidance schemes based on fuzzy logic have been developed for a planar engagement model, with randomly jinking target maneuver and line-of-sight (LOS) rate measurement corrupted with glint noise. Two versions of fuzzy guidance schemes have been proposed, the first one using information required for proportional navigation (PN) and the second one using the information required for augmented PN(APN). The performance of the two fuzzy guidance schemes, in terms of commanded acceleration profiles and the values of the terminal miss distance, have been compared with PN and APN, respectively. It is observed that the fuzzy guidance schemes are able to match closely the performance of PN and APN guidance laws, and in cases where the measurements are noisy and the estimates are inaccurate, the fuzzy guidance schemes are shown to perform better than PN and APN.

Fuzzy-Logic-Based Homing Guidance Schemes

The guidance schemes based on fuzzy logic presented here differ in terms of the input variables required for their implementation.

Scheme 1: Proportional Navigation Based

The PN guidance law requires closing velocity V_c and LOS rate $\dot{\lambda}$ information. Using these two measurements, the first fuzzy guidance scheme (FGS-1) has been developed.

The input and output variables of a fuzzy system are called linguistic variables, as they take linguistic values (e.g., large, small, very large, small positive, large negative, etc.). The input linguistic variables of FGS-1 are P $(= V_c\dot{\lambda})$ and PC $(=$ *change in* $P = P_{\text{present}} - P_{\text{previous}})$ and the output variable is a_C (commanded acceleration). The normalized universe of discourse for all of the above three linguistic variables is $[-1, +1]$.

The linguistic values taken by these variables are expressed by linguistic sets. Each of the above-mentioned three linguistic variables is assumed to take seven linguistic values as defined:

LN = large negative
LP = large positive
MN = medium negative
MP = medium positive
SN = small negative
SP = small positive
ZE = zero

The linguistic sets are described by their membership functions. For simplicity, triangular membership functions as described in Ref. 1 have been used. Apart from the above linguistic sets, one more linguistic set, ANY, has been assumed for all the three variables. ANY has a membership function of 1.0 at every element.[1]

In fuzzy logic control, system behavior is characterized by a set of linguistic rules. These rules usually take the form IF (antecedent) THEN (consequent) and can be derived from different sources.[2] A great deal of experimentation and trial and error are needed to firm up on the final set of rules. After some experimentation, a set of 15

Received May 26, 1993; revision received Nov. 8, 1993; accepted for publication Nov. 11, 1993.

*Graduate Student, Department of Computer Science and Automation.
†Professor, Department of Computer Science and Automation.
‡Scientist, Advanced Technology Program.